Journal of Physics:
Conference Series

PURPOSE-LED PUBLISHING™

PAPER • **OPEN ACCESS**

Validation of real-weather LES using SCADA data from a large modern offshore wind farm

To cite this article: R de Jong *et al* 2026 *J. Phys.: Conf. Ser.* **3224** 032003

View the article online for updates and enhancements.

You may also like

- Comparing methods for coupling wake models to an atmospheric perturbation model in WAYVE
Koen Devesse, Sebastiano Stipa, Joshua Brinkerhoff et al.
- Large-eddy simulations of wind farm production and long distance wakes
O Eriksson, K Nilsson, S-P Breton et al.
- Extension and Validation of Minimalistic Prediction Model to Determine the Energy Production of Offshore Wind Farms
Jens N. Sørensen, Ariadna M. I. Garcia, Gunner C. Larsen et al.

SmarAct | group

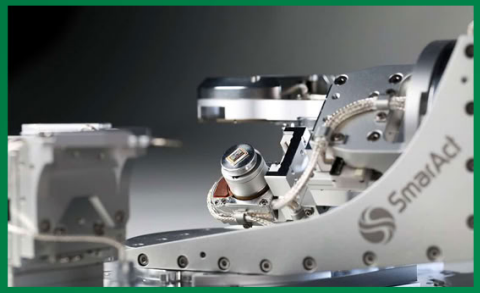
More details and registration

webinar

One sample, many dimensions: prospects for multimodal nanoscale characterization

Explore how precise sample manipulation enables complementary nanoscale techniques to work together on one sample

Live at 2 p.m. GMT/3 p.m. CET,
12 November 2026



This content was downloaded from IP address 31.151.17.97 on 13/11/2026 at 19:31

Journal of Physics: Conference Series **3224** (2026) 032003 doi:10.1088/1742-6596/3224/3/032003

Validation of real-weather LES using SCADA data from a large modern offshore wind farm

R de Jong[1], B M Doekemeijer[2], J J Kreeft[2], R A Verzijlbergh[1] and J W van Wingerden[1]

[1] Delft University of Technology, Delft, The Netherlands
[2] Shell Global Solutions International B.V., The Hague, The Netherlands

E-mail: r.dejong-1@tudelft.nl

Abstract. Wake interactions between turbines become increasingly more complex as offshore wind farms grow in size and are built in closer proximity to one another. This increased complexity challenges the accuracy of steady-state wake models for estimating Annual Energy Production (AEP). Atmospheric Simulation Platform for Innovation, Research, and Education (ASPIRE), a real-weather Large-Eddy Simulation (LES) model, offers a promising alternative. While ASPIRE has been validated for free-stream wind conditions, its validation for AEP estimation remains limited due to the scarcity of publicly available power data. This study validates ASPIRE for AEP estimation using two years of 5-minute SCADA data from the large modern offshore wind farm Hollandse Kust Noord and benchmarks ASPIRE's performance against several steady-state wake models. The results show that ASPIRE outperforms steady-state wake models in estimating AEP, albeit at a higher computational cost. The ASPIRE model achieves a significantly lower AEP error of 0.96% compared to 3.38% for the best-performing steady-state wake model, Cumulative Curl. The ASPIRE model also has the lowest wake loss error at 0.25 percentage points compared to 0.34 for Cumulative Curl. Furthermore, with the chosen grid resolution, ASPIRE underperforms for single-wake cases, but performs well when a turbine is waked by multiple upstream turbines or experiences free-stream flow, which accounts for the majority of operating situations. These results demonstrate that real-weather LES improves AEP estimation accuracy compared to steady-state wake models for the Hollandse Kust Noord wind farm, making it a valuable tool for wind farm development.

1. Introduction

The capacity of offshore wind is expanding rapidly. The European Union has set targets to increase the offshore wind capacity from 16.3 GW in 2022, to 60 GW in 2030 and 300 GW in 2050 [1]. To achieve these goals, newly constructed wind farms are larger and are being built in closer proximity to other wind farms, especially in the North Sea [2]. As a consequence, the flow dynamics in and around wind farms are becoming increasingly complex, and turbines there are subject to more pronounced wake effects from surrounding turbines [3].

Steady-state wake models are often used to model these wake effects, especially for estimating Annual Energy Production (AEP), where higher-fidelity wake models are usually too computationally expensive. However, these models are highly sensitive to the site-specific input parameters, leading to uncertainty in their estimations when field data are unavailable for calibration [4].

Content from this work may be used under the terms of the Creative Commons Attribution 4.0 licence. Any further distribution of this work must maintain attribution to the author(s) and the title of the work, journal citation and DOI.
Published under licence by IOP Publishing Ltd

This is often the case during the design and construction phases of a wind farm, when AEP estimates are most critical, or when assessing the influence of future neighboring wind farms. There are many possible higher fidelity wake models that could improve the accuracy of the AEP estimation [5]. In this paper, real-weather Large-Eddy Simulation (LES) is further investigated.

The Atmospheric Simulation Platform for Innovation, Research, and Education (ASPIRE) model facilitates AEP estimation with real-weather LES. Time-varying global atmospheric reanalysis data are used as input for the simulation, ensuring that large-scale atmospheric conditions are taken into account. Furthermore, the model is GPU-based, which significantly increases computational performance [6]. The ASPIRE model has been validated for free-stream wind conditions using meteorological mast data [7] and Light Detection And Ranging (LiDAR) data [8]. Although validation for wind conditions within a wind farm is more complex, this has been demonstrated for the Borssele wind farm zone [8].

Validating ASPIRE for AEP remains a challenge. This is primarily due to the lack of publicly available power data, which are often commercially sensitive [8]. Modeled and measured hourly wind farm power data are compared for a few Belgian offshore wind farms; however, the data quality limits the study to a sanity check rather than a quantitative validation [8]. Moreover, in-house wind farm power validation has been performed by Whiffle [9]. Nevertheless, the availability of public ASPIRE validation using power data remains very limited.

In this study, ASPIRE is validated for AEP using two years of 5-minute Supervisory Control And Data Acquisition (SCADA) data from the large modern offshore wind farm Hollandse Kust Noord (HKN). These SCADA data are compared with results from a corresponding real-weather LES. Besides assessing the AEP, an analysis of wake loss, power per wind bin, and power ratio is performed to investigate the underlying causes of the AEP error. Furthermore, several steady-state wake models are included as benchmarks. In doing so, this work validates ASPIRE for AEP estimation at HKN and offers a comparison against widely used steady-state wake models.

2. Methods

This section outlines the data, models, and analysis methods used in this study. Section 2.1 describes the content and postprocessing of the SCADA data. Section 2.2 presents the real-weather LES setup. Section 2.3 explains the use of the steady-state wake models. Section 2.4 details the application of FLORIS-Based Analysis for SCADA Data (FLASC), and Section 2.5 defines the evaluation metrics (AEP error, wake loss error, power error, and power ratio).

2.1. SCADA data

This study uses 5-minute SCADA data collected from January 2024 to December 2025 at HKN, which is a wind farm located in the Dutch North Sea. The SCADA data contain the measured turbine power, wind speed, and wind direction for each turbine within HKN. The HKN wind farm, which became operational in December 2023, consists of 69 wind turbines, each rated at 11 MW with a rotor diameter of 200 meters [10]. Prior to comparison, data points with missing measurements, invalid measurements, curtailed turbines, or power outliers are discarded. A northing calibration is applied to correct the wind-direction measurements. Furthermore, when a data point from a turbine is removed, any downstream turbines significantly affected by its wake at that time are also excluded. In total, 52% of the SCADA data points are considered valid, and only these data points are used in the analysis. Finally, a free-stream wind direction and free-stream wind speed are assigned to each data point. The free-stream wind direction is determined from the farm-wide average wind direction. Subsequently, the free-stream wind speed is computed by averaging the wind speeds from the upstream turbines in the wind farm.

2.2. Real-weather LES

The HKN wind farm was simulated using ASPIRE, an LES model operated by Whiffle, covering the period from January 2024 to December 2025. A uniform Actuator Disk Model (ADM) was used to model the turbines in both the LES and the mesoscale simulation. In addition to HKN, the simulation includes the neighboring wind farms Prinses Amaliawindpark, Egmond aan Zee, Eneco Luchterduinen, and Hollandse Kust Zuid, each modeled using their respective power curves. The layout and locations of these wind farms are shown in Figure 1.

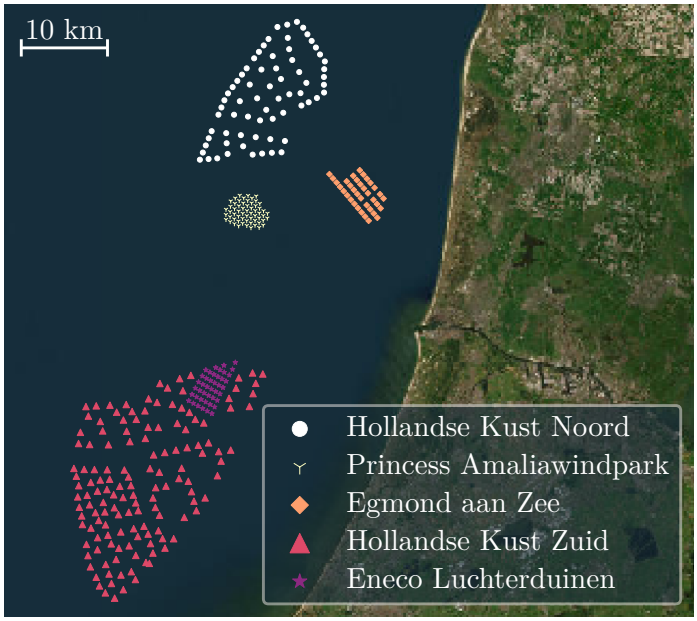


Figure 1. Location and layout of the wind farms surrounding HKN, located in the Dutch North Sea [2].

Table 1. Listed are the grid resolutions $(\Delta x, \Delta y, \Delta z)$, the domain dimensions (L_x, L_y, L_z), and the number of grid cells (N_x, N_y, N_z) in each spacial direction, and the vertical grid stretching parameters $(\Delta z_0, z_c, z_g : \Delta z = \Delta z_0 + z_g \cdot \max\{z - z_c, 0\})$.

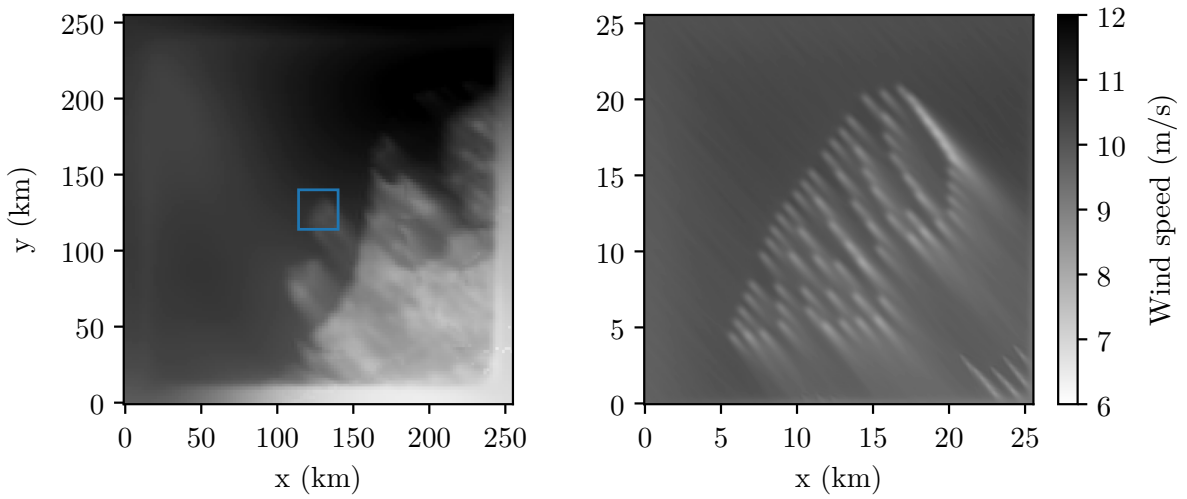
	mesoscale domain	LES domain
Δx	2000 m	100 m
Δy	2000 m	100 m
Δz	$[50, 290]$ m	$[25, 79]$ m
L_x	256 km	25.6 km
L_y	256 km	25.6 km
L_z	5 km	3 km
N_x	128	256
N_y	128	256
N_z	39	71
Δz_0	50 m	25 m
z_c	150 m	325 m
z_g	0.05	0.02

The simulation setup consists of two nested domains. A mesoscale simulation is performed using the European centre for medium-range weather forecasts ReAnalysis v5 (ERA5) dataset as input. Within this domain, a higher resolution LES is conducted. Figure 2 illustrates the two nested domains by showing horizontal slices at hub height of the average wind speed for a single day simulated with ASPIRE. The simulation domain settings are listed in Table 1. The vertical grid resolution is stretched. It starts at Δz_0, then from z_c it grows with z_g at each step.

The two-year simulation period is divided into individual daily segments, each treated as an independent simulation that can be executed in parallel. Each daily segment includes a spin-up period of 6 hours for the mesoscale simulation and 1 hour for the LES. The model time step, Δt, is determined dynamically during the simulation to satisfy numerical stability constraints for advection and diffusion processes. It is defined as:

$$\Delta t = \min\left(\Delta t_{max}, C \min_i\left(\frac{\Delta x_i}{u_i}\right), Pe \min_i\left(\frac{\Delta x_i}{\nu_t}\right)\right),$$

where Δx_i denotes the grid-cell size, u_i the maximum velocity present in the domain, and ν_t the eddy diffusivity. For the LES, the maximum time step $\Delta t_{\max}$, Courant number C, and Peclet number Pe are set to 20 s, 1.2, and 0.5, respectively, whereas for the mesoscale simulation these values are set to 120 s, 0.8, and 0.3.



(a) A slice of the meso-scale simulation showing the wakes of the wind farms and the lower wind speeds above the Netherlands. The blue square indicates the LES domain within the mesoscale domain.

(b) A slice of the LES simulation showing the individual turbine wakes of the HKN wind farm and of a few turbines from neighboring wind farms Prinses Amaliawindpark and Egmond aan Zee.

Figure 2. Horizontal slices at hub height showing the average wind speed for a single day simulated with ASPIRE. The meso simulation is shown on the left and the LES simulation on the right.

After the simulation, real-weather LES data points corresponding to missing or removed SCADA data points are discarded as well. The free-stream wind direction and free-stream wind speed are assigned to each data point using the same procedure as for the SCADA dataset.

2.3. Steady-state wake models

In addition to the real-weather LES, the SCADA data are compared against several steady-state wake models available in FLOw Redirection and Induction in Steady State (FLORIS) [11]. These include Cumulative Curl (CC), Gauss Curl Hybrid (GCH), Empirical Gaussian (Emgauss), Jensen, and Turbulence Optimised Park (TurbOPark). All steady-state wake models are evaluated using the submodels and corresponding default parameters specified in Table 2, which can also be found on the FLORIS GitHub page [11]. Unless otherwise specified, the FLORIS base model is used. In selected cases, FLORIS' uncertainty model is applied as well. This model introduces wind-direction uncertainty by performing a Gaussian blending of results from multiple nearby wind directions. A wind-direction uncertainty of 10° corresponds to a standard deviation of 10° in the Gaussian distribution. For each FLORIS model, a lookup table is generated, where the turbine powers are computed for many combinations of wind speed, wind direction, and turbulence intensity. The turbulence intensities are set based on the average ambient turbulence intensity measured by the IJmuiden met-mast on the Dutch North Sea [12] for the data point's free-stream wind speed.

2.4. Data postprocessing with FLASC

All postprocessing is performed using the FLASC tool [13], following the SMARTEOLE examples 1-4, with the following minor adjustments. The curtailment filtering step is adjusted for the HKN turbine, classifying a measurement as curtailed when the power output is more than 1 MW below the rated power while operating above the rated wind speed. The FLORIS lookup tables are computed at finer resolutions of 1° in wind direction, 0.5 m/s in wind speed, and 0.02 in turbulence intensity.

Table 2. Steady-state wake models available in FLORIS with their combination model (Sum of Squares Freestream Superposition (SOSFS) or Freestream Linear Superposition (FLS)), turbulence model, and velocity model specified.

Model	Combination	Turbulence	Velocity
Jensen	SOSFS	Crespo-Hernandez initial = 0.1, constant = 0.5, ai = 0.8, downstream = -0.32	Jensen we = 0.05
GCH	SOSFS	Crespo-Hernandez initial = 0.1, constant = 0.5, ai = 0.8, downstream = -0.32	Gauss alpha = 0.58, beta = 0.077, k_a = 0.38, k_b = 0.004
Emgauss	SOSFS	Wake Induced Mixing atmospheric_ti_gain = 0.0	Emperical Gauss wake_expansion_rates = [0.023,0.008], breakpoints_D = 10, sigma_0_D = 0.28, smoothing_D = 2.0, mixing_gain_velocity = 2.0
CC	SOSFS	Crespo-Hernandez initial = 0.01, constant = 0.9, ai = 0.83, downstream = -0.25	CC a_s = 0.179367259, b_s = 0.0118889215, c_s1 = 0.0563691592, c_s2 = 0.13290157, a_f = 3.11, b_f = -0.68, c_f = 2.41, alpha_mod = 1.0
TurbOPark	FLS	Crespo-Hernandez initial = 0.1, constant = 0.5, ai = 0.8, downstream = -0.32	TurbOPark A = 0.04, sigma_max_rel = 4.0

The analysis follows the procedure described in SMARTEOLE Example 12 [13]. First, the LES time series is binned using the function `bin_timeseries_to_grid`, producing a table containing the mean power production and the number of samples for each turbine, wind direction bin, and wind speed bin. Next, the LES and FLORIS tables are mapped onto the SCADA time series using `interpolate_floris_from_df_approx`. Based on these mapped time series, the AEP error is computed using `compare_cumulative_production`, and the wake-loss error is evaluated using `compare_relative_wake_loss`. To compute power errors, the mapped time series are converted back into tabular form using `bin_timeseries_to_grid`. The resulting table allows the metrics defined in subsection 2.5 to be applied. Finally, the power ratio including all wind speeds is calculated using `compute_energy_ratio`.

2.5. Metrics

Four performance metrics are used to evaluate the agreement between the model estimations and the SCADA data. Each mapped time series χ consists of the power of each turbine τ at time t. All data points, $P_\tau(\chi, t)$, are first grouped into wind bins defined by wind direction, θ, and wind speed, v. The turbine power of each wind bin, $P_\tau(\chi, \theta, v)$, is computed as the mean of all power data points belonging to that turbine and wind bin. The number of data points available for a turbine in a given wind bin is used as the weight, $w(\tau, \theta, v)$.

The first metric is the relative AEP error, $\varepsilon_{\mathrm{AEP}}(\chi)$, defined as:

$$\varepsilon_{\mathrm{AEP}}(\chi) = \frac{\mathrm{AEP}(\chi) - \mathrm{AEP(SCADA)}}{\mathrm{AEP(SCADA)}} \times 100\%. \tag{1}$$

The AEP is proportional to the cumulative farm energy, $E_{cum}(\chi)$, defined as:

$$E_{cum}(\chi) = \sum_t \sum_\tau P_\tau(\chi, t).$$

The second metric is wake loss error, $\varepsilon_{\mathrm{WL}}(\chi)$, defined as:

$$\varepsilon_{\mathrm{WL}}(\chi) = \mathrm{WL}(\chi) - \mathrm{WL}(\mathrm{SCADA}). \tag{2}$$

Here, the wake loss, $\mathrm{WL}(\chi)$, is defined as:

$$\mathrm{WL}(\chi) = \frac{\sum_t \sum_\tau P_{\mathrm{upstream}}(\chi, t) - \sum_t \sum_\tau P_\tau(\chi, t)}{\sum_t \sum_\tau P_{\mathrm{upstream}}(\chi, t)} \times 100\%,$$

with $P_{\mathrm{upstream}}(\chi, t)$ being the mean power of the upstream turbines.
The third metric is the power error, $\varepsilon_P(\chi, \theta, v)$, defined as:

$$\varepsilon_P(\chi, \theta, v) = \frac{P_{farm}(\chi, \theta, v) - P_{farm}(\mathrm{SCADA}, \theta, v)}{P_{farm}(\mathrm{SCADA})} \times 100\%. \tag{3}$$

Here, the farm power, $P_{farm}(\chi, \theta, v)$, is defined as:

$$P_{farm}(\chi, \theta, v) = \sum_\tau P_\tau(\chi, \theta, v) \cdot \frac{w(\tau, \theta, v)}{\tilde{w}(\theta, v)},$$

where the normalized weight, $\tilde{w}(\theta, v)$, is defined as:

$$\tilde{w}(\theta, v) = \frac{\sum_\tau w(\tau, \theta, v)}{\sum_\theta \sum_v \sum_\tau w(\tau, \theta, v)}.$$

The SCADA farm power, $P_{farm}(\mathrm{SCADA})$, is a constant value defined as:

$$P_{farm}(\mathrm{SCADA}) = \sum_\theta \sum_v \sum_\tau P_\tau(\mathrm{SCADA}, \theta, v) \cdot w(\tau, \theta, v).$$

The power errors are combined by computing the weighted mean, weighted mean absolute, and mean absolute values, called WM, WMA, and MA respectively, defined as:

$$\mathrm{WM}(\chi) = \sum_\theta \sum_v \tilde{w}(\theta, v) \times \varepsilon_P(\chi, \theta, v),$$
$$\mathrm{WMA}(\chi) = \sum_\theta \sum_v \tilde{w}(\theta, v) \times |\varepsilon_P(\chi, \theta, v)|,$$
$$\mathrm{MA}(\chi) = \frac{1}{|\theta| \cdot |v|} \times \sum_\theta \sum_v |\varepsilon_P(\chi, \theta, v)|.$$

The fourth metric is the power ratio of a turbine, $\mathcal{R}_\tau(\chi, \theta, v)$, defined as:

$$\mathcal{R}_\tau(\chi, \theta, v) = \frac{P_\tau(\chi, \theta, v)}{P_{\mathrm{upstream}}(\chi, \theta, v)}. \tag{4}$$

When a metric is shown only per wind direction bin, it means that all wind speeds are grouped into one large bin.

3. Results

This section presents the performance of the ASPIRE and steady-state models. Section 3.1 compares the AEP error and wake loss error across all models, followed by a comparison of their computational cost in Section 3.2. Section 3.3 decomposes the power error, Section 3.4 examines the power error per wind bin, and Section 3.5 compares turbine-level power ratios across different wind directions.

3.1. AEP error and wake loss error

To compare the AEP errors and wake loss errors of the different models, a statistical analysis is performed. The errors were computed by comparing one year of SCADA data with one year of modeled data. Bootstrapping was applied by sliding a one-year window across a 2-year dataset in weekly steps, yielding 52 error samples per model. A comparison between all models shows that ASPIRE has a significantly lower AEP error than any of the steady-state wake models. As illustrated in Figure 3, ASPIRE achieves a median AEP error of 0.96%, whereas the best-performing steady-state wake model, CC, attains a median AEP error of 3.38%. Similarly, ASPIRE produces the lowest wake-loss error, at 0.25 percentage points (p.p.). However, the difference with the best-performing steady-state wake model, CC, which has a wake loss error of 0.34 p.p., is relatively small. These results indicate that the steady-state wake models tend to overestimate the power production not only of waked turbines but also of upstream turbines. For the steady-state wake models, the impact of the wind-direction uncertainty of up to 10° was investigated as well. However, the impact was minimal. For CC, the median AEP error decreased by at most 0.19 p.p., whereas the wake loss error increased.

The higher AEP error for the steady-state wake models can be explained by several assumptions. For example, it is assumed that the wind speeds reported in the SCADA data are correct, and that the upstream turbines accurately capture the free-stream wind speed. When using this free-stream wind speed as input for the steady-state wake models, the blockage effect and the influence of neighboring wind farms are ignored. It is also assumed that the turbine power curve is perfect and that no operational losses occur. The wake loss metric normalizes against the upstream turbines to mitigate these effects. Furthermore, the steady-state wake models assume homogeneous flow throughout the wind farm, constant wind conditions without any veer or shear, and perfect yaw alignment with the incoming wind direction. ASPIRE does capture these dynamic behaviors.

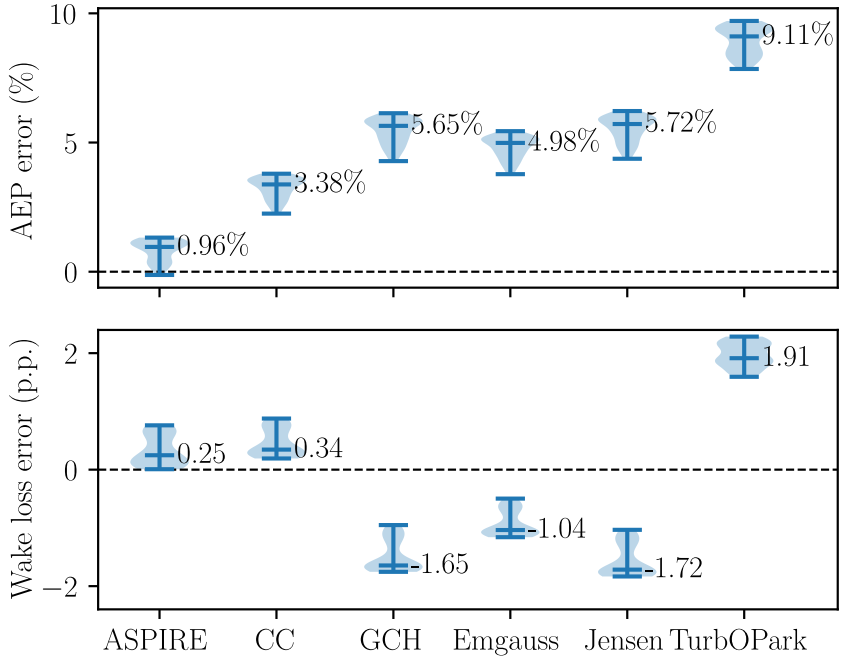


Figure 3. AEP error distributions and wake loss error distributions for the real-weather LES model ASPIRE and several steady-state wake models. Horizontal blue lines denote the extrema and the median, with the median also indicated explicitly.

Table 3. Computation time for AEP estimation corresponding to a full-year simulation on a single GPU for ASPIRE and generating a table of turbine power values for 61,560 different wind conditions on a single CPU for the steady-state wake models.

Model	Time (h)
ASPIRE	54
CC	3.0
GCH	0.63
Emgauss	0.21
Jensen	0.064
TurbOPark	0.064

3.2. Computational cost

The computational cost of real-weather LES is substantially higher than that of the steady-state wake models (see Table 3). Simulating a single day of the HKN wind farm with ASPIRE, given the chosen setup, required an average of 537 seconds on a single *NVIDIA GeForce RTX 3090* GPU. With a multi-GPU setup, these simulations can be executed in parallel, meaning that the total wall-clock time for simulating a full year depends strongly on the number of GPUs available. The computational cost also depends strongly on the chosen grid resolution. For the steady-state wake models, the computational expense is dominated by the generation of a lookup table of turbine power values. In this study, the table was computed on a single *13th Gen Intel(R) Core(TM) i7-1365U* CPU for 360 wind directions, 57 wind speeds, and 3 turbulence intensities. These calculations can also be parallelized, which significantly reduces the wall-clock time. Furthermore, the computational cost depends on the number of wind conditions chosen for the table. Ultimately, real-weather LES may not be feasible for all applications. However, it could be well-suited for cases where accurate AEP estimation is critical.

3.3. Power error decomposition

To further investigate the sources of the AEP errors, the weighted mean, weighted mean absolute, and mean absolute values of the power errors over all wind bins are compared in Figure 4. These power errors are based on the full two years of data. Note that the weighted mean power error is equivalent to the AEP error. The weighted mean absolute value of the ASPIRE power errors is considerably larger than the weighted mean value, indicating substantial cancelation between positive and negative power errors. Interestingly, the difference between the mean absolute values of both CC and ASPIRE is much smaller than the difference observed for their weighted mean values. This suggests that CC may achieve performance close to that of ASPIRE under individual wind conditions. When analyzing the AEP error per turbine, significantly higher errors occur on the southeast side of the wind farm for both ASPIRE and CC. On the western border, ASPIRE even underestimates the power. The difference becomes evident when the AEP error is split into two parts corresponding to the northwest and southeast sides of the wind farm, as shown in Figure 5.

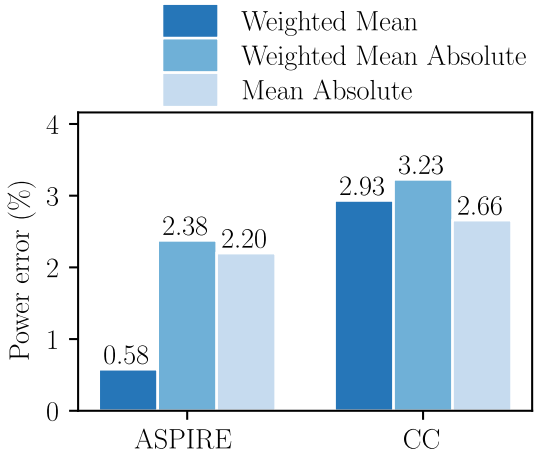


Figure 4. The weighted mean, weighted mean absolute, and mean absolute values of the power errors over all wind bins for the ASPIRE and CC models.

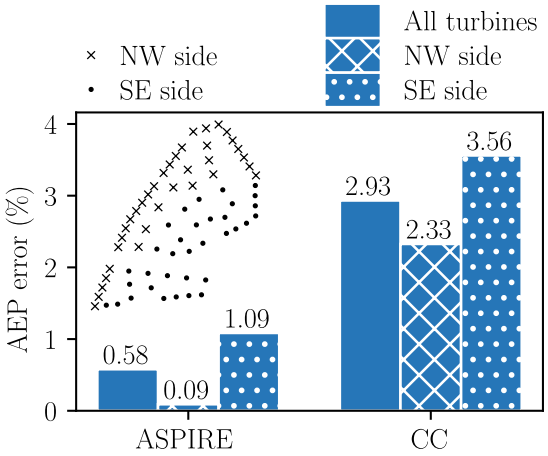


Figure 5. The AEP error for the ASPIRE and CC model with respect to the SCADA data of the full wind farm, the northwest (NW) side, and the southeast (SE) side.

3.4. Power error per wind bin

When the power error is analyzed as a function of wind speed, significant errors are observed only well above cut-in and below rated wind speeds. This is expected, as the power curve is steepest in this region. When the power error is examined as a function of wind direction, CC tends to consistently overestimate power production, whereas ASPIRE shows both over- and underestimation depending on the wind direction. The largest errors for CC occur when the wind farm is aligned with the incoming wind, around 45° and 225°, as shown in Figure 6. In these regions, the ASPIRE model performs substantially better. This suggests that CC may struggle to correctly model long-distance wake effects and cumulative wake interactions, whereas ASPIRE captures these effects more accurately.

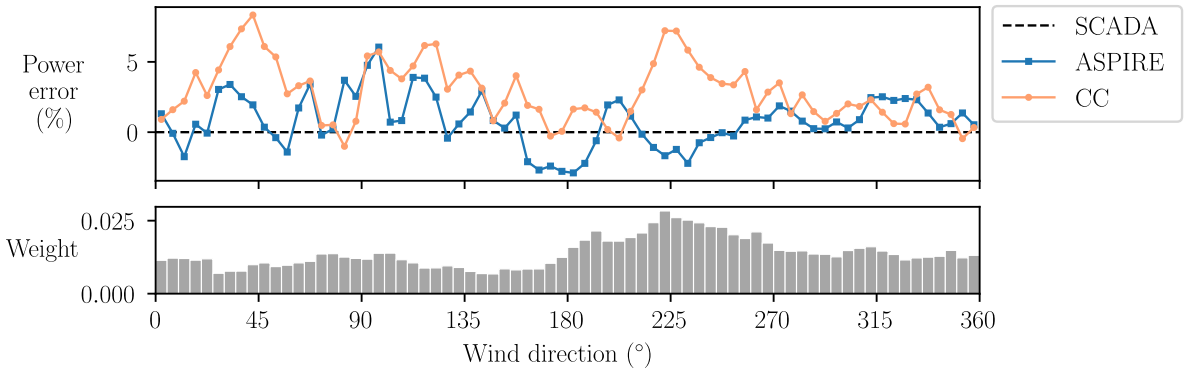


Figure 6. Power error per wind-direction bin for ASPIRE and CC with respect to the SCADA data, alongside the number of SCADA data points per wind-direction bin.

3.5. Power ratio

Wake interactions were further examined by analyzing the power ratio between turbine 1 (the most southwestern turbine) and the mean power of the upstream turbines for each wind-direction bin (see Figure 7). For the CC model, the power ratio is shown both with a wind-direction uncertainty of 10° (CC 10°) and without wind-direction uncertainty (CC 0°). At 21.5° and 84.8°, turbine 1 is waked by an array of upstream turbines, resulting in large dips in the observed power ratio. Between these wind directions, the turbine remains within the wind farm's wake, yielding ratios below one, whereas outside these wind directions, it receives free-stream wind. The CC model substantially overestimates the power loss caused by an array of upstream turbines at 21.5° and 84.8°. Adding wind-direction uncertainty reduces the deficit at the wake center but smears the deficit across adjacent bins, leading to approximately the same power overall. Around 205°, the upstream turbines on the western side produce more power than the upstream turbines on the eastern side. The ASPIRE model captures the heterogeneous inflow caused by an upstream wind farm, whereas CC does not. Because turbine 1 is on the west side of the wind farm, its power ratio becomes higher than one for the SCADA data and ASPIRE model at 205°.

Opposed to turbine 1, ASPIRE does not significantly outperform CC for turbine 2 in terms of AEP. The AEP errors for turbine 1 are 0.46% with ASPIRE, 1.58% with CC 10°, and 1.73% with CC 0°, whereas for turbine 2 they are 1.40%, 1.28% and 1.47% respectively. When analyzing the power ratio of turbine 2, the ASPIRE model especially shows larger errors when the turbine is waked by a single upstream turbine at 137.5° and 201.5°. The coarse LES grid tends to smear the wake, causing wake-center wind speeds to be overestimated and wake-edge wind speeds to be underestimated. When turbine 2 is waked by an array of wind turbines at 21.5°, ASPIRE does

produce accurate power ratios. Overall, both turbines show accurate estimations with ASPIRE when they experience wake effects from multiple upstream turbines or free-stream flow. The primary limitation arises when a turbine is directly behind a single upstream turbine. The accuracy could likely be improved by using a finer grid resolution for the LES; however, this would substantially increase the computational cost.

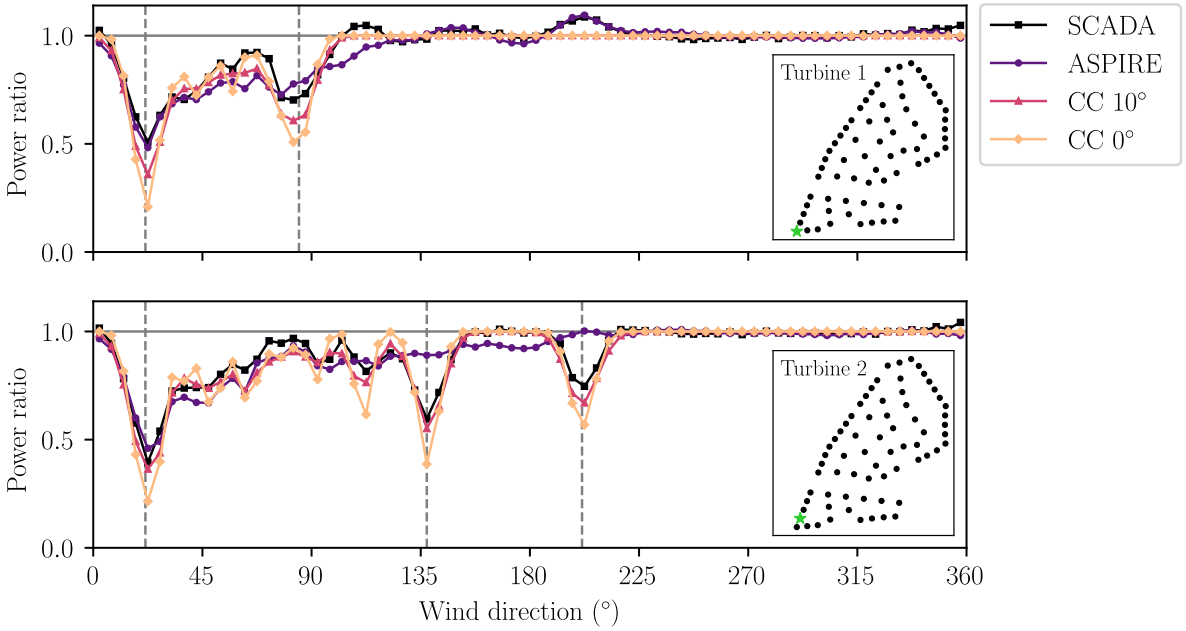


Figure 7. Ratios between the power of turbine 1 (top) and turbine 2 (bottom) with respect to the mean power of the upstream turbines for each wind-direction bin. The power ratios from the SCADA data and the models ASPIRE, CC 10° (with wind-direction uncertainty), and CC 0° (without wind-direction uncertainty) are shown. The vertical gray lines indicate when the turbine is waked by a close turbine upstream. The green star on the map indicates the location of the turbine within the HKN wind farm.

4. Conclusion

This study validates the real-weather LES model ASPIRE for AEP estimation using SCADA data from the HKN wind farm and benchmarks it against the uncalibrated steady-state wake models CC, GCH, Emgauss, Jensen, and TurbOPark. The ASPIRE model achieves a median AEP error of 0.96%, substantially outperforming the best steady-state model, CC, with a median AEP error of 3.38%. The wake loss error is 0.25 p.p. for ASPIRE and 0.34 p.p. for CC. However, these gains come with a higher computational cost. The models diverge most when the wind farm is aligned with the incoming wind, where ASPIRE clearly outperforms CC. The ASPIRE model tends to underperform when a turbine is directly in the wake of a single upstream turbine, a limitation attributed to the coarse grid resolution. In contrast, ASPIRE predicts power accurately when turbines are subject to multiple overlapping wakes or free-stream flow, which accounts for the majority of operating situations. Overall, the results demonstrate that real-weather LES improves the AEP estimation accuracy over steady-state wake models for the HKN wind farm, highlighting its value as a reliable tool for wind farm development. Extending this analysis to additional wind farms will help assess the generality of these findings.

5. Acknowledgments

This work is part of the Hollandse Kust Noord wind farm innovation program, where CrossWind C.V., Shell, Grow, Eneco and Siemens Gamesa are teaming up; funding for the PhDs was provided by CrossWind C.V. and Siemens Gamesa. Further, this work has been supported by the SUDOCO project, which receives funding from the European Union's Horizon Europe Programme under the grant agreement No. 101122256.

References

[1] European Commission 2023 Delivering on the EU offshore renewable energy ambitions https://eur-lex.europa.eu/legal-content/EN/TXT/?uri=celex:52023DC0668

[2] 4C-Offshore Global offshore map https://map.4coffshore.com/offshorewind/ (Accessed on 2025-12-01)

[3] Baas P 2024 Winds of the North Sea in 2050 - Public Final Report https://wins50.nl/downloads/wins50_endreport_final_20240403.pdf

[4] Keim J A 2024 Analysis of engineering wake model validation and calibration with historical data from OWEZ wind farm https://resolver.tudelft.nl/uuid:8b483b8b-d1cd-4983-8198-fde756114a8a

[5] Amiri M M, Shadman M and Estefen S F 2024 A review of physical and numerical modeling techniques for horizontal-axis wind turbine wakes *Renewable and Sustainable Energy Reviews* **193** 114279 https://doi.org/10.1016/J.RSER.2024.114279

[6] Schalkwijk J, Jonker H J, Siebesma A P and Meijgaard E V 2015 Weather Forecasting Using GPU-Based Large-Eddy Simulations *Bulletin of the American Meteorological Society* **96**(5) 715–723 https://doi.org/10.1175/BAMS-D-14-00114.1

[7] Baas P, Verzijlbergh R, Dorp P V and Jonker H 2023 Investigating energy production and wake losses of multi-gigawatt offshore wind farms with atmospheric large-eddy simulation *Wind Energy Science* **8** 787–805 https://doi.org/10.5194/wes-8-787-2023

[8] Baas P, Verzijlbergh R and Dorp P V 2024 21GW Roadmap Wake Study: Model Validation Report https://offshorewind.rvo.nl/file/download/8690c7fb-a571-43e6-8e38-ceeeb5ded7a2/20241212_rvo_wakestudy_validation_f.pdf

[9] van Dorp P and The Whiffle Team 2025 Multi-year, time series-based validation of a real weather, meso-scale coupled large eddy simulation (LES) of wind farm power production for 10 operational wind farms https://whiffle.nl/wp-content/uploads/20250325_pim_van_dorp_wind_europe_going_beyond_the_mean.pdf

[10] Crosswind Het windpark https://www.crosswindhkn.nl/nl/windpark/ (Accessed on 2025-12-01)

[11] NLR FLORIS Version 4.4.1 https://github.com/NatLabRockies/floris/tree/main/examples/inputs (Accessed on 2026-02-18)

[12] TNO Offshore Wind Measurements MeteoMast IJmuiden https://offshorewind-measurements.tno.nl/meetlocaties/meteomast-ijmuiden-mmij/ (Accessed on 2025-12-01)

[13] NLR FLASC Version 2.5 https://github.com/NatLabRockies/flasc/tree/main/examples_smarteole (Accessed on 2026-03-12)